RSC Advances

PAPER

View Article Online
View Journal | View Issue

Cite this: *RSC Adv.*, 2019, **9**, 16007

Protective effects of the flavonoid fraction obtained from pomelo fruitlets through ultrasonic-associated microwave extraction against AAPH-induced erythrocyte hemolysis†

Qin Wang,[b] Jieying Luo,[b] Huifan Liu,*[b] Charles Stephen Brennan,[d] Jianliang Liu[c] and Xiaoyu Zou[a]

Received 3rd April 2019
Accepted 6th May 2019

DOI: 10.1039/c9ra02523e

rsc.li/rsc-advances

Pomelo fruitlet is a side-product of pomelo, and this study aimed to extract the antioxidative flavonoid compounds from pomelo fruitlets with high efficiency through ultrasonic-associated microwave methods. Scanning electron microscopy analysis indicated that the spatial structure of the pomelo fruitlet powder was changed; microwaves and ultrasonic waves facilitated the formation of globular and curved surfaces, respectively. Ultrasonic-microwave synergistic pretreatment resulted in significantly higher yield. Each type of flavonoid compound was characterized using PR-LCMS analysis, and naringin with high nutritive value was detected in all groups. After purifying the flavone fractions with AB-8 macroporous resin, naringin, 2″-*O*-acetyl-3′-*O*-methylrutin, and 5,7,8,3′-tetrahydroxy-3,4′-dimethoxy were identified, which could act as free radical scavengers to protect erythrocytes from AAPH-induced hemolysis. This study strongly improved the effects of ultrasonic-microwave synergetic methods on the high utilization of pomelo fruitlets, especially in terms of flavonoid extraction and bioavailability.

1. Introduction

Flavonoids are known to have several medicinal uses;[1] for example, they can work as antioxidant and enzyme inhibitors, promote heart and blood vessel health, protect the liver, and aid in estrogen replacement, muscle relaxation, and nerve relaxation. Nowadays, studies on flavonoids in grapefruit mainly focus on the peel and juice. Examples of studies in this area are an appraisal method for the composition and content of flavonoids in grapefruit,[2,3] investigation of different varieties of flavonoids and antioxidant activity in pomelo,[4] influence of the flavonoid content in grapefruit on physiological regulating mechanisms,[5,6] effect of grapefruit flavonoids on gene expression,[7,8] modulation of grapefruit flavonoid content during the process of production, storage, and processing,[9,10] research on the absorption of grapefruit flavonoids,[11,12] grapefruit flavonoid biosynthesis,[13,14] research on the effects of grapefruit flavonoid extracts on weight control,[15] grapefruit flavonoid and drug interactions,[16] and the like. However, there are very few studies on the golden pomelo, which is a specialty fruit of Lingnan and currently abundantly harvested in South China, especially in Meizhou City in Guangdong Province. Owing to its excellent flavor and high nutritional value, large quantities of golden pomelo are now exported to the United States, Canada, Europe, and other countries. During the natural growth of the plant, low percentage of fruit settings causes pomelo fruitlets to be formed, which are immature pomelo fruits. The yield of the pomelo fruit litter is high, but the utilization of this fruit resource is often ignored. Therefore, it is immensely important to make full use of pomelo fruitlets to protect the environment and improve the comprehensive utilization value of the golden pomelo.

At present, the extraction methods of flavonoids mainly include organic solvent extraction, acid precipitation, supercritical fluid extraction, ultrasonic-assisted extraction, and microwave-assisted extraction. The high energy effect of microwaves can lead to cell membrane rupture, accelerate the dissolution of substances inside cells, and intensify molecular movement. Therefore, microwave power is an important factor affecting the extraction rate of flavonoids. The cavitation of ultrasound can cause cell rupture, and the agitation and oscillation produced by ultrasound make up for the shortcomings of microwaves, such as uneven mass transfer and

[a]*Sericultural and Agri-Food Research Institute, Guangdong Academy of Agricultural Sciences, Key Laboratory of Functional Foods, Ministry of Agriculture and Rural Affairs, Guangdong Key Laboratory of Agricultural Products Processing, China*
[b]*College of Light Industry and Food, Zhongkai University of Agriculture and Engineering, Guangzhou, Guangdong 510225, China. E-mail: lm_zkng@163.com*
[c]*Modern Agriculture Research Center, Zhongkai University of Agriculture and Engineering, Guangzhou, Guangdong 510225, China*
[d]*Department of Food, Wine and Molecular Biosciences, University of Lincoln, Christchurch, New Zealand*

† Electronic supplementary information (ESI) available. See DOI: 10.1039/c9ra02523e

heat transfer. Our previous study optimized the extraction conditions for pomelo fruitlets and the final predictive equation was obtained as follows:

$$Y = 68.57 + 5.2A + 5.38B + 4.39C + 4.8D - 3.22AB - 1.12AC - 3.45AD - 2.55BC + 0.5765BD - 1.56CD - 18.24A^2 - 12.47B^2 - 15.13C^2 - 12.75D^2$$

where A is the microwave power (W), B is the power of the ultrasonic wave (W), C is the ratio of the material to the solvent (g mL^{-1}), and D is the extraction time (min). The optimum conditions for the extraction of flavonoids from pomelo fruitlets were a material-to-solvent ratio of 1 : 11, extraction time of 42 min, microwave power of 410 W, and ultrasonic wave power of 420 W, and the extraction efficiency was 68.57 ± 2.43%.

Subsequently, this study was performed to promote the comprehensive utilization of the golden pomelo crop by exploring the functional potential of its fruitlets, which have always been considered an unusable side product. The aims of this study are to (a) explore the effects of microwaves and ultrasonic waves on flavonoid extraction from pomelo fruitlets; (b) explain how the extraction methods, especially the synergistic effect of the microwave and ultrasonic technologies, affect the spatial structure, the extraction yield, the compositions of the extracted flavonoid compound fractions, and the antioxidative capabilities; and (c) purify the flavonoid fraction *via* AB-8 macroporous resin and characterize its structure-related protective mechanism against AAPH-induced erythrocyte hemolysis. This study may provide some useful information on the utilization of pomelo fruitlets and the extraction process of flavonoid compounds with high efficiency.

2. Materials and methods

2.1 Materials

Pomelo fruitlets were collected from the GAP farm in Meizhou City, Guangdong Province, China. Human blood samples were collected from three healthy adult volunteers. Vitamin C (VC), AAPH, DPPH, and ABTS were purchased from Sigma-Aldrich (St Louis, MO, USA). Phosphate-buffered saline (PBS; pH 7.4) was purchased from Gibco Life Technologies (Grand Island, NY, USA). Kits to determine the GSH-Px, SOD, and LDH activities and the MDA, T-GSH, GSSG, and H_2O_2 contents were purchased from Beyotime Institute of Biotechnology (Shanghai, China). Sodium hydroxide, anhydrous ethanol, diethyl alcohol, potassium persulfate, sodium dihydrogen phosphate dihydrate, disodium hydrogen phosphate dodecahydrate, potassium ferrocyanide, trichloroacetic acid, ferric chloride, and other chemicals and reagents used were of analytical grade and commercially available.

2.2 Pomelo fruitlet powder preparation

Pomelo fruitlets were chopped into small pieces (1–3 cm each) and were lyophilized (FD-1A-50, Beijing Boyikang Laboratory Instruments Co. Ltd, China). The dried pomelo fruitlet pieces were crushed in a high-speed mill (high-speed multifunctional pulverizer, Yongkang Baoou Hardware Products Co. Ltd, China) into powder. The powder was passed through 60 meshes and stored at 4 °C until use.

2.3 Extraction of total flavonoid content

The detailed processes of the extraction methods are listed below and the main differences are presented in Table 1.

Water bath (named as the WB group): take 1.00–3.00 g of the pomelo fruitlet powder and condition by soaking in 60% ethanol solution with liquid ratio of 20 : 1 for 30 min. The temperature of water is 60 °C.

Microwave alone (named as the M400 group): soak 1.00–3.00 g of pomelo fruitlet powder in 60% ethanol with liquid ratio of 20 : 1 under 400 W microwave power for 40 min. The extraction temperature is maintained at 60 °C and the ultrasonic power is always 0.

Ultrasonic waves alone (named as the U400 group): soak 1.00–3.00 g of the pomelo fruitlet powder in 60% ethanol with liquid ratio of 20 : 1 under 400 W ultrasonic power. The extraction temperature is maintained at approximately 60 °C for 40 min and the microwave power is 0.

Ultrasonic-associated microwave: soak 1.00–3.00 g of pomelo fruitlet powder in 60% ethanol with liquid ratio of 20 : 1. The extraction temperature is maintained at approximately 60 °C. The sample groups are subject to various ultrasonic and microwave powers, as shown in Table 1. As can be seen, the groups named as M100+U400, M400+U100, and M400+U400 were treated with 100 W of microwave and 400 W of ultrasonic power, 400 W of microwave and 100 W of ultrasonic power, and 400 W of microwave and 400 W of ultrasonic power, respectively, for 30 min or 40 min. The M400 → U400 group was first treated with microwaves for 15 min and then with ultrasonic waves for 15 min, whereas the U400 → M400 group was treated in the reverse manner.

The extraction rate of the total flavonoid content was calculated as

$$R(\%) = \frac{c \times N \times V_1 \times V_2}{m \times V_3} \times 100\%$$

where R (%) represents the total flavonoid yield, c (mg L^{-1}) represents the total flavonoid concentration of the sample, N represents the dilution ratio of the extract, m (g) represents the quantity of the freeze-dried grapefruit powder, V_1 (mL) represents the volume of the extracted liquid, V_2 (mL) represents the constant volume of the liquid to be tested, and V_3 (mL) represents the volume of the sample liquid.

After processing with the different extraction methods, the sample solutions were centrifuged at 1900 × g for 10 min; the supernatant (named as cCF) was lyophilized and stored at −40 °C until use. The sediment was dried at 60 °C until its weight did not change. It was subsequently stored at 4 °C until use.

2.4 Purification of flavonoid compounds

The crude flavone fraction (cCF) was obtained after lyophilization from the group pretreated with ultrasonic waves (400

Table 1 The conditions of the extraction of flavonoid compounds from pomelo fruitlets and corresponding treatments

Extraction method	Sample name	Microwave power (W)	Ultrasonic wave power (W)	Time (min)
Water bath alone	WB	0	0	30
Microwave alone	M400	400	0	40
Ultrasonic alone	U400	0	400	40
Ultrasonic associated with microwave	M100+U400	100	400	40
	M400+U100	400	100	40
	M400+U400	400	400	30 or 40
	M400→U400	400	400	M15→U15
	U400→M400	400	400	U15→M15

W) associated with microwaves (400 W) for 40 min. A total of 0.024 g of cCF was dissolved in 100 mL of ultrapure water, filtered through 0.22 μm microporous filters, loaded onto AB-8 macroporous resin (2.5 × 40 cm^2), and then eluted at a flow rate of 3 mL min^{-1} with 600 mL each of ultrapure water and 40% ethyl alcohol sequentially. Following elution and lyophilization, the flavonoid fraction, P-F, was obtained. The content was evaluated as described above, and the yield of purified flavone fraction, CF, was calculated as follows:

$$\text{CF yield}(\%) = \frac{\text{Flavonoid weight in P-F}}{\text{Flavonoid weight before purification}} \times 100\%$$

2.5 Scanning electron microscopy (SEM) analysis

The spatial structures of the sediment comprising the pomelo fruitlets were analyzed after treatment by the various methods shown in Table 1. Before performing SEM (Zeiss Supra55, Zeiss, China), the variously treated pomelo fruitlets were prepared by metal spraying.

2.6 Composition analysis of flavonoid compounds by PR-LCMS

Freeze-dried flavone samples extracted by the different methods were dissolved in methanol and analyzed by PR-LCMS. Chromatography for the liquid-phase condition was performed using a Shimadzu PR-LCMS-2020 with an Inert-Sustain C18 column of dimensions 4.6 × 150 mm and the mobile phase as acetonitrile–water–0.1% formic acid gradient elution. The column temperature was 40 °C, flow rate was 0.3 mL min^{-1}, and the injection volume was 1 μL. The mass spectrometry conditions were the ion mode of EIS^+, capillary voltage of 3.98 kV, taper hole voltage of 40 V, ion source temperature of 100 °C, peeling agent temperature of 300 °C, quality range in m/z, photomultiplier voltage of 80 V, and gas flow of 49 L h^{-1}.

2.7 Determination of chemical antioxidant properties

2.7.1 Estimation of DPPH radical scavenging activity (DRSA). The DRSA was assessed according to a previously reported method[17] with some modifications. Briefly, 1 mL of all the flavonoid compound sample solutions with different treatments (10, 20, 30, 40, and 50 μg mL^{-1}) was added to 3 mL DPPH (0.1 mmol L^{-1}) and mixed thoroughly. The mixture was reacted at room temperature for 30 min in the dark. DPPH solution with VC was used as the positive control group. The absorbance was measured at 517 nm and the DRSA was calculated using the following formula:

$$\text{DRSA}(\%) = \frac{A_C - A_S}{A_C} \times 100$$

where A_C and A_S are the absorbance values of the control and sample groups, respectively. The DRSA of the four fractions was analyzed by comparison with the concentration of the sample that caused a 50% reduction in the DPPH radicals.

2.7.2 Estimation of ABTS radical scavenging activity. The ABTS radical scavenging activity was measured using a previously reported method[18] with some modifications. The working solution was 7.4 mM ABTS stock solution with an equivolume of 2.6 mM potassium persulfate, which was reacted for 12 h in the dark. The absorbance value of the diluted ABTS working solution was 0.7 ± 0.02 at 734 nm, which was obtained with PBS. Then, 0.2 mL of the flavonoid compound sample solutions with different treatments (10, 20, 30, 40, and 50 μg mL^{-1}) was added to 2 mL diluted ABTS working solution to form the sample groups. The ABTS solution with VC was used as the positive control group. The mixture was reacted for exactly 6 min at room temperature in the dark, and the absorbance was measured at 734 nm. The ABTS radical scavenging activity was subsequently calculated using the following equation:

$$\text{ABTS radical scavenging activity}(\%) = \frac{A_C - A_S}{A_C} \times 100$$

where A_C and A_S are the absorbance values of the control and sample groups, respectively.

2.7.3 Estimation of FRAP. Briefly, 1 mL of the variously treated flavonoid compound sample solutions (10, 20, 30, 40, and 50 μg mL^{-1}) was diluted with 1 mL of 0.2 M phosphate buffer. The diluted samples were mixed with 1 mL of 1% potassium ferricyanide, incubated at 50 °C for 20 min, and then 1 mL of 10% trichloroacetic acid was added for 10 min to stop the reaction. Then, 1 mL of the reaction solution was added to 1 mL of distilled water and 1 mL of 0.1% $FeCl_3$ for 10 min at room temperature. After centrifugation for 10 min at 1200 × g, the absorbance of the supernatant was measured at 700 nm. VC was used as the positive control.[19]

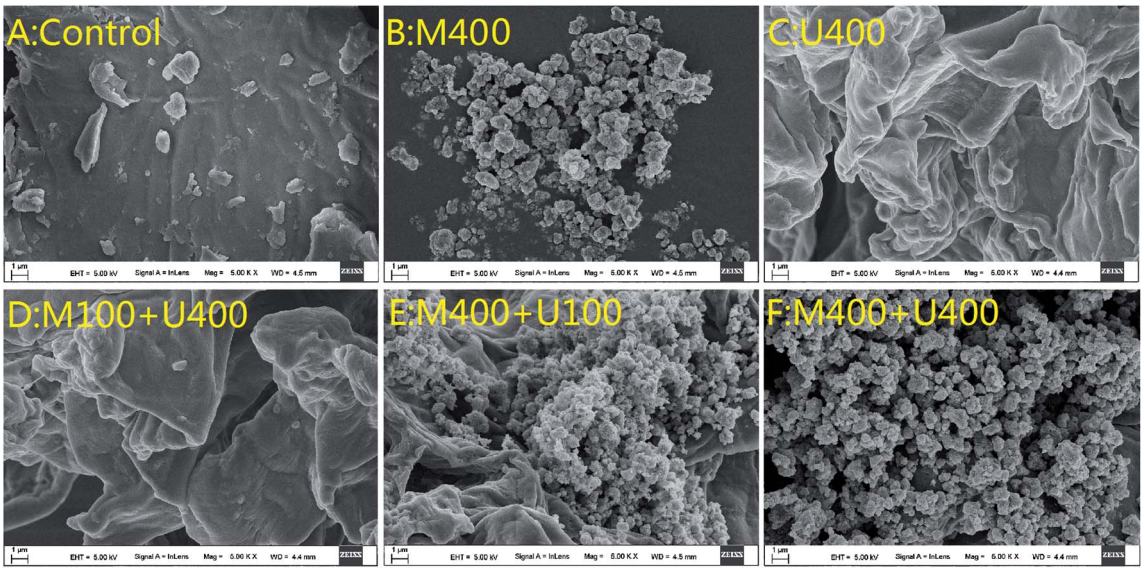

Fig. 1 SEM micrographs (5000×): (A) pomelo fruitlet powder; (B) the M400 group; (C) the U400 group; (D) the M100+U400 group; (E) the M400+U100 group; (F) the M400+U400 group.

2.8 Determination of erythrocyte hemolysis induced by AAPH

2.8.1 Determination of AAPH-induced erythrocyte hemolysis rate. Erythrocytes were obtained from blood samples by washing them thrice with PBS (pH 7.4) by centrifugation (1200 × *g*, 10 min, 4 °C). The erythrocyte suspensions were diluted 4-fold with PBS (pH 7.4) and then 200 μL of the freeze-dried flavone samples extracted by different methods was added to 200 μL PBS and to the variously treated flavonoid compound sample solutions (50 μg mL^{-1}). The mixtures were incubated for 30 min at 37 °C and 400 μL of 0.2 mM AAPH was added, followed by incubation for another 2 h with gentle shaking. Subsequently, the well-incubated mixture was diluted with 3.2 mL of PBS (pH 7.4) and centrifuged (1200 × *g*, 10 min, 4 °C). The absorbance of the supernatant was measured at 540 nm, similar to the treated sample groups. Ultrapure water was added to the above suspension to obtain 100% hemolysis. The hemolysis inhibition rate was calculated as follows:

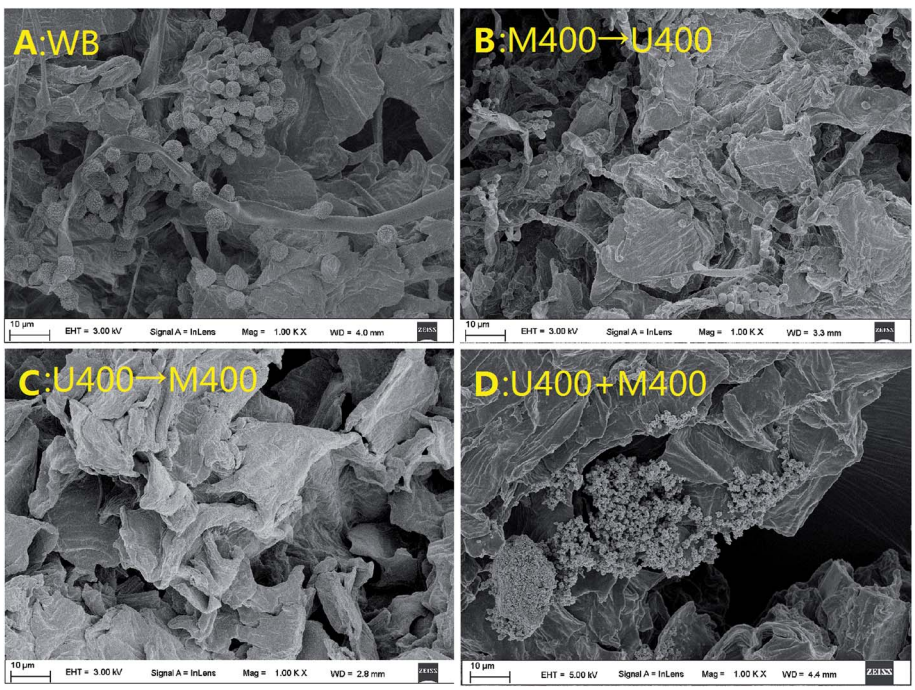

Fig. 2 SEM micrographs (5000×): (A) the WB group; (B) the M400→U400 group; (C) the U400→M400 group; (D) the M400+U400 group.

Table 2 The extraction efficiency and hemolysis rate of flavonoids compounds from pomelo fruitlets after different treatments

Sample name	Microwave power (W)	Ultrasonic wave power (W)	Time (min)	Extraction efficiency[a] (%)	Hemolysis rate[a] (%)
Water bath	0	0	30	23.81 ± 2.51 a	30.21 ± 0.05 b,c
M400	400	0	40	30.28 ± 2.01 b	30.03 ± 0.16 b,c
U400	0	400	40	29.03 ± 1.62 b	28.82 ± 0.13 a,b,c
M100+U400	100	400	40	59.80 ± 2.70 c	28.65 ± 0.18 a,b,c
M400+U100	400	100	40	55.56 ± 1.62 c	27.08 ± 0.20 a
M400+U400	400	400	40	68.20 ± 1.59 d	26.56 ± 0.05 a
M400→U400	400	400	M15→U15	29.70 ± 3.68 b	33.85 ± 0.18 c
U400→M400	400	400	U15→M15	20.66 ± 2.41 a	31.25 ± 0.13 d
M400+U400	400	400	30	56.35 ± 4.28 c	28.16 ± 0.05 a,b

[a] Data are expressed as mean ± standard deviation. The letters following each value in the same line indicate significant differences at $p < 0.05$.

$$\text{Hemolysis rate}(\%) = \frac{\text{OD}_{540} \text{ of sample treated group}}{\text{OD}_{540} \text{ of } 100\% \text{ hemolysis}} \times 100$$

2.8.2 Determination of MDA, GSH-Px, T-GSH, GSSG, SOD, H_2O_2, and LDH. Erythrocytes were obtained as described previously, but the supernatant was discarded after 3 washes with PBS (pH 7.4) and the erythrocytes were added to double ultrapure water in an ice-water bath for 10 min and then centrifuged (1200 × *g*, 10 min, 4 °C) to obtain the cell lysis buffer. The SOD, GSH, and GSSG contents were determined using GSH and microscale SOD kits. A cellular glutathione peroxidase kit, total superoxide dismutase assay kit, malondialdehyde kit, and lactate dehydrogenase kit were used to determine the GSH-Px, H_2O_2, MDA, and LDH activities, respectively.

2.9 Statistical analysis

The data were expressed as the mean ± standard deviation of three replicates. Significant differences between the means of different parameters were calculated with Duncan's multiple-range test using Statistical Package for the Social Sciences (SPSS) 17.0 software (SPSS Inc., Chicago, IL, USA). The differences were considered statistically significant at $P < 0.05$.

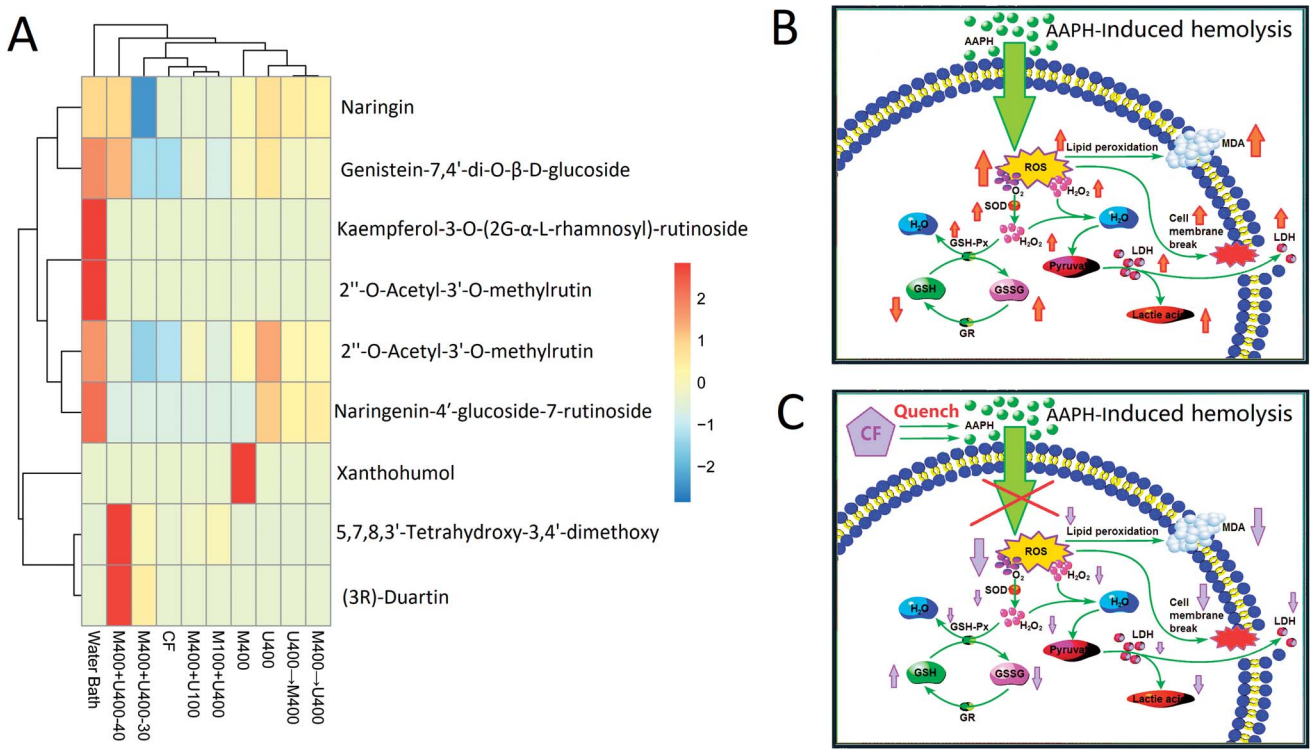

Fig. 3 (A) Heat maps for the cluster analysis of the types of flavones in each pretreatment group. (B) The ROS level increased when AAPH free radicals induced erythrocyte hemolysis and the corresponding changes in the antioxidative associated enzyme activities and the metabolite content. (C) The possible intracellular antioxidant-detoxifying mechanisms of CF sample attenuating AAPH-induced oxidative stress by inhibiting ROS generation.

3. Results and discussions

3.1 Spatial structure of pomelo fruitlets after various pretreatments

Several studies have reported that both microwaves and ultrasonic waves introduce destructive changes in extracted samples, mainly because of the cavitation effect of the ultrasonic waves and the high-energy effect of the microwaves.[20,21] These destructive changes include increasing temperature and pressure inside the cellular tissue, which results in a structure variation. Therefore, this study first characterized the spatial structure *via* SEM analysis. The results for the different pretreatments are shown in Fig. 1. Without any treatment, the pomelo powder under a scanning electron microscope of 5000× magnification appeared as a flat surface with some fragments superposed on the surface (Fig. 1A). However, after treatment with various methods, the flat surface disappeared and a complex spatial structure was formed. In detail, after treatment with microwaves alone (400 W, 40 min), dense globules were observed, which tended to aggregate on the surface (Fig. 1B). Transmitted as waves, microwaves are able to penetrate biomaterials and interact with polar molecules in the biomaterials to generate heat, resulting in the formation of globules.[22] When the sample was treated with ultrasonic waves alone (400 W, 40 min), as shown in Fig. 1C, no globule-like shape was observed. However, a curved surface with irregularities was observed, which might have been because of cavity collapse due to the sound waves.[23] When treated with ultrasonic-associated microwaves, the group showed a higher percentage of the spatial structure corresponding to waves with higher power. The spatial structures in the group treated with 100 W microwaves and 400 W ultrasonic waves mainly showed the curved surface with very few globules (Fig. 1D), whereas the group treated with 400 W microwaves and 100 W ultrasonic waves showed globules with less curving of the surface (Fig. 1E). However, under 400 W microwaves and 400 W ultrasonic waves, the spatial structure of the pomelo fruitlets showed only the aggregation of the globules (Fig. 1F), which was very similar to that seen in the M400 group. In order to determine the reason for this, microwaved and ultrasonic waved of the same power were applied to the sample but the total treatment time was reduced from 40 min to 30 min; the results are presented in Fig. 2. When the extraction time was decreased to 30 min, the spatial structure of the pomelo fruitlets in the U400+M400 group with 400 W microwaves and 400 W ultrasonic waves showed a combination of globules and curved surfaces (Fig. 2D), indicating that the extraction time was a determining factor in the formation of the spatial structure. The U400→M400 group, which received only ultrasonic wave treatment for the first 15 min followed by only microwave treatment for the next 15 min, showed only the curved surface on the pomelo fruitlet powder, as depicted in Fig. 2C. We determined that the curved surfaces were the effects of the high power of the ultrasonic waves, which disrupted the formation of globules, although the microwave power was equally strong at 400 W. Fig. 2A shows the spatial structure after the water bath treatment at 60 °C for 30 min, which displays a curved surface mixed with saturated spheres with many bulges on the surface. This specific spherical shape was very similar to that of the 400M group and the M400→U400 group (as shown in Fig. 2B). We inferred that a high temperature resulted in the formation of such globules. In summary, we inferred that the processing time, temperature, power of the waves, and the processing method are important factors that affect the formation of the spatial structure.

3.2 Flavonoid extraction yield of pomelo fruitlets after different pretreatments

Technology based on cell wall breakdown is key to obtaining high yield and extraction efficiency from natural compounds.[24] In this study, the effects of the processing order and the power of microwaves and ultrasonic waves on the extraction yields of the total flavonoid compounds were analyzed. As shown in Table 2, the extraction efficiencies of the water bath group at 60 °C and the U400→M400 group were the lowest; the values for these two groups showed no significant differences. When treated with 400 W ultrasonic waves (U400 group) or microwaves (M400 group), the extraction yields of the flavonoid compounds were significantly higher, the tendencies of which were the same as for the M400→U400 group. However, the synergetic effects of the ultrasonic waves and microwaves on the extraction yield of the flavonoid compounds from the pomelo fruitlets were promising, as the extraction efficiencies of the M100+U400 group, M400+U100 group, and M400+U400 (30 min) group increased significantly; especially, the M400+U400 (40 min) group showed the highest efficiency (68.20 ± 1.59%). Therefore, we could conclude that both microwave and ultrasonic wave treatments enhance the effective extraction of the flavonoid compounds. With regard to the spatial structure of the pomelo fruitlets, the treatment groups with relatively low extraction yield showed a curved surface in their spatial structures, whereas the yield increased with increasing percentage of the globular structure induced mainly by microwaves, in which both power and processing time had a positive effect on the extraction efficiency. The polar substances, especially the water molecules inside the cell wall, are able to translate the microwave energy into thermal energy, and the very high temperature finally results in the destruction of the cell integrity, which facilitates the entry of the extracellular solvents into the cell to dissolve and release the intracellular bioactive compounds.[25] Therefore, we inferred that the globular structure resulted from the destruction of the cell integrity, induced by the effects of microwaves on the pomelo fruitlets, which increased the possibility of extracting solvents contacting the intracellular flavonoid compounds. Apart from the high possibility of the extracellular solvents entering the cell wall, the globular structure could also enlarge the contact area, which led to high extraction efficiency.

Moreover, in this study, we found the order of processing with ultrasonic waves and microwaves had a very slight effect on increasing the extraction yield. The U400→M400 group, which was subject to ultrasonic waves (400 W for 15 min) prior to microwaves (400 W for 15 min), showed significantly lower extraction yield than the M400→U400 group. This result was very interesting, as there were no significant differences between the M400, U40, and M400→U400 groups. We concluded that the result might be because of the synergistic

Table 3 The characteristic description of the flavone compositions in the CF sample group based on PR-LCMS analysis

Chemical component	Chemical formula	Retention time (min)	*m/z*	Error	Response value
Naringin	$C_{27}H_{32}O_{14}$	3.18	581.1868	0.3	369 165
2″-*O*-Acetyl-3′-*O*-methylrutin	$C_{30}H_{34}O_{17}$	3.38	667.1888	1.9	36 131
5,7,8,3′-Tetrahydroxy-3,4′-dimethoxy	$C_{17}H_{14}O_8$	3.56	347.0746	−1.6	8162

action of the microwaves and ultrasonic waves, which plays a significant role in increasing the yield, but the sequence of the ultrasonic and microwave treatment was inconsequential. Because the curved surface with no globular structures was observed in the U400→M400 group (as seen in Fig. 2C) whereas the M100+U400 group showed fewer globular structures (as seen in Fig. 1D), we concluded that the formation of the curved surface delayed the generation of the globular structure to some extent and consequently lowered the extraction efficiency. Wang *et al.* extracted selenium polysaccharide from selenium-rich tea by a microwave-ultrasonic synergistic method, where the extraction rate of selenium polysaccharide reached 4.56%.[26] Guo *et al.* used a microwave-ultrasonic combined extraction method to improve the extraction efficiency and economic benefits of cochineal dye, and the extraction efficiency was 4 times that of the traditional method.[27] Qiao *et al.* considered the flavonoid content as an index to optimize the microwave-ultrasonic extraction process of the total flavonoid content from folium xylose, and found that this method had the advantages of high extraction rate, short extraction time, and small ethanol consumption, which made it an effective method to extract the total flavonoid content.[28]

3.3 Analysis of flavonoid compositions with different extraction methods

To further explore the effects of ultrasonic wave and microwave treatments on the extraction of flavonoid compounds from pomelo fruitlets, PR-LCMS analysis was employed in this study to analyze the compositions of the flavonoid compounds in each extracted sample. Information such as the retention time, fragment profiles, errors and response value, and the chemical formula are characterized and the corresponding chemical

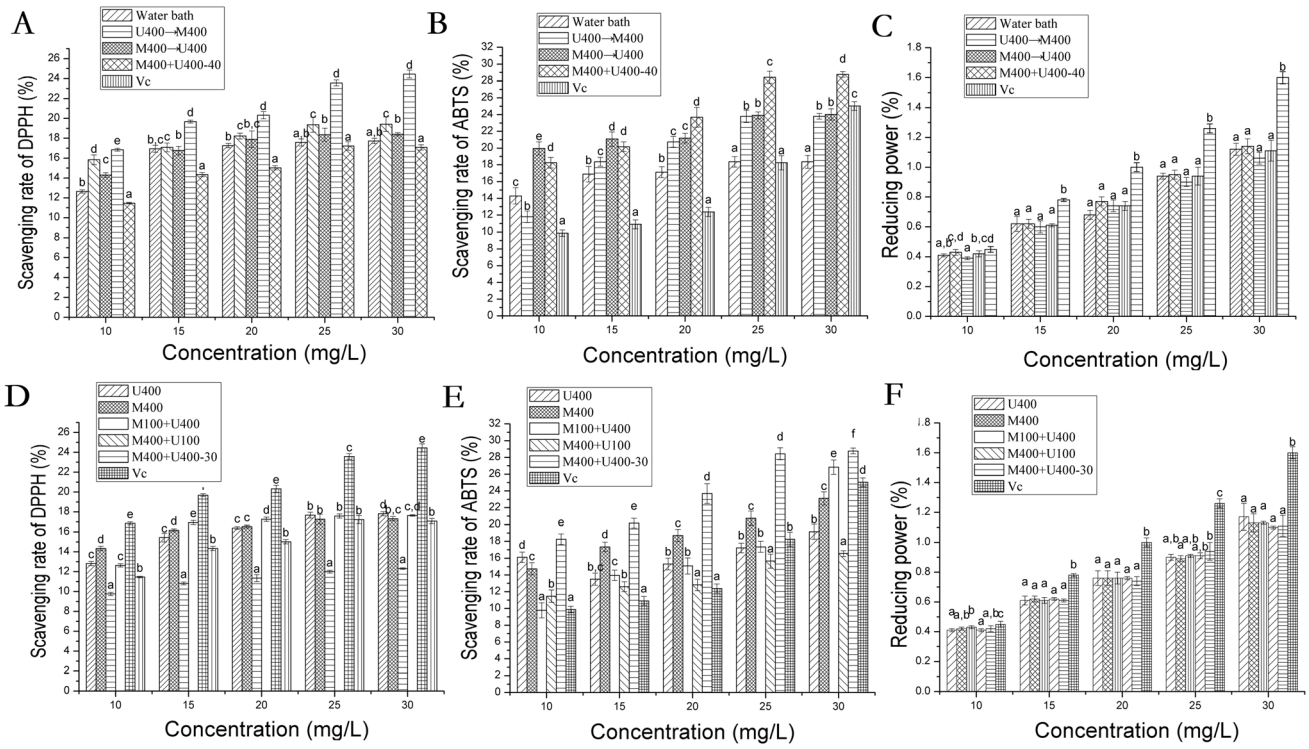

Fig. 4 Scavenging abilities of the extracted flavonoid compounds including the group treated with water bath alone, the M400→U400 group, the U400→M400 group, and the M400+U400 group: (A) DPPH and (B) ABTS free radicals. (C) Ferric ion reducing antioxidative power and the scavenging abilities of the extracted flavonoid compounds including the M400 group; the U400 group; the M100+U400 group; the M400+U100 group; and the M400+U400 group for (D) DPPH and (E) ABTS free radicals. (F) Ferric ion reducing antioxidative power. VC groups were the positive control groups. Data are expressed as the mean ± standard deviation. For each measurement, the data labeled with different letters were significantly different ($p < 0.05$).

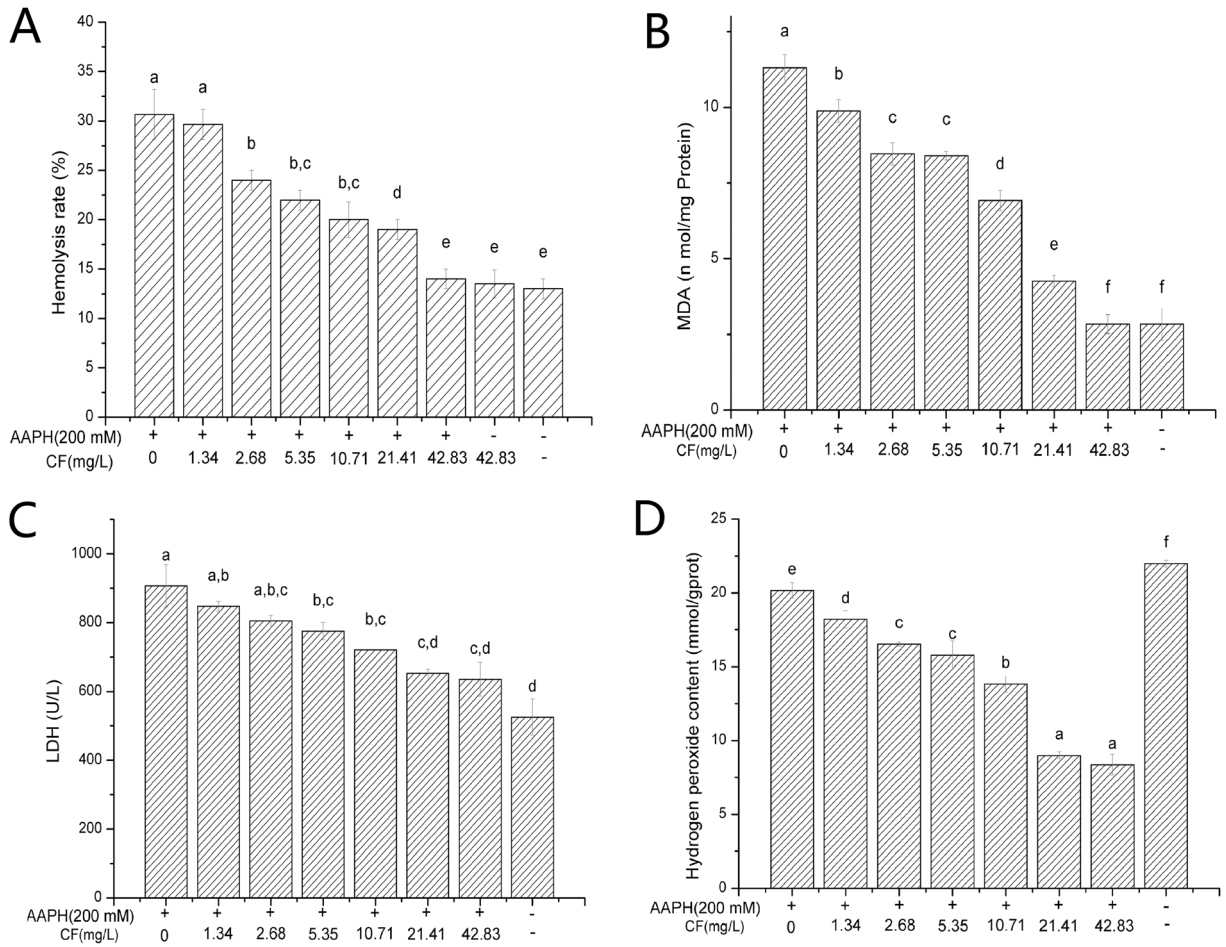

Fig. 5 (A) Inhibitory activity of CF sample on AAPH-induced ROS overexpression in human erythrocytes. Changes in MDA content (B), the enzyme activities of LDH (C), and hydrogen peroxide content (D). Erythrocytes were pretreated with CF sample for 30 min prior to AAPH (200 mM) treatment for 2 h. Data are mean ± standard deviations of three independent experiments.

components of the flavonoid compounds in all treatment groups are described in the ESI s-Tables 1–9.† It can be seen that the extraction yield has a weak relation with the diversity of the flavonoids. For example, the WB group with relatively low extraction efficiency contained the most types of flavonoid compounds, which was a total of 6, whereas the group M400+U400 (40 min) with the highest extraction yield contained 5 types of flavonoid compounds. With synergistic treatments of the same power, the processing time could also affect the secondary structure profiles of the flavonoid compounds. Naringin and 2″-*O*-acetyl-3′-*O*-methylrutin were detectable in all treatment groups. Naringin is a flavanone-7-*O*-glycoside between the flavanone naringenin and the disaccharide neohesperidose. The flavonoids naringenin and hesperetin, which form the aglycones of naringin and hesperidin, occur naturally in citrus fruits, especially in grapefruit, where naringin is responsible for the bitter taste of the fruit. Naringin inhibits some drug-metabolizing cytochrome P450 enzymes, including CYP3A4 and CYP1A2, which may result in drug–drug interactions.[29,30] Ingestion of naringin and related flavonoids can also affect the intestinal absorption of certain drugs, leading to an increase or decrease in the circulating drug levels. The consumption of citrus (especially grapefruit) and other juices with medications is contraindicated to avoid interference with drug absorption and metabolism. Various other pharmacological effects have been observed *in vitro* or in animal studies, but their relevance to human health is unknown. These effects include the following: naringin is an inhibitor of vascular endothelial growth factor release, which causes angiogenesis.[31] 2″-*O*-Acetyl-3′-*O*-methylrutin is a derivative of rutin. It has been reported to inhibit aldose reductase and platelet aggregation.[32] Furthermore, we found that 5,7,8,3′-tetrahydroxy-3,4′-dimethoxy flavone was only identified in the groups with ultrasonic-associated microwave extraction, which included the M400+U100, M100+U400, M400+U400-30, and M400+U400-40 treatment groups. This result indicated that the synergistic effect of ultrasonic-associated microwave treatment had great impact on the types of extracted flavones. No current literature is available on the specific structure of 5,7,8,3′-tetrahydroxy-3,4′-dimethoxy flavone, whereas it has been reported that a similar structure can affect superoxide production and tyrosine phosphorylation of protein.[33,34] Through the cluster analysis shown in Fig. 3, we could deduce that the processing time not only affected the extraction yield, but also determined the types and

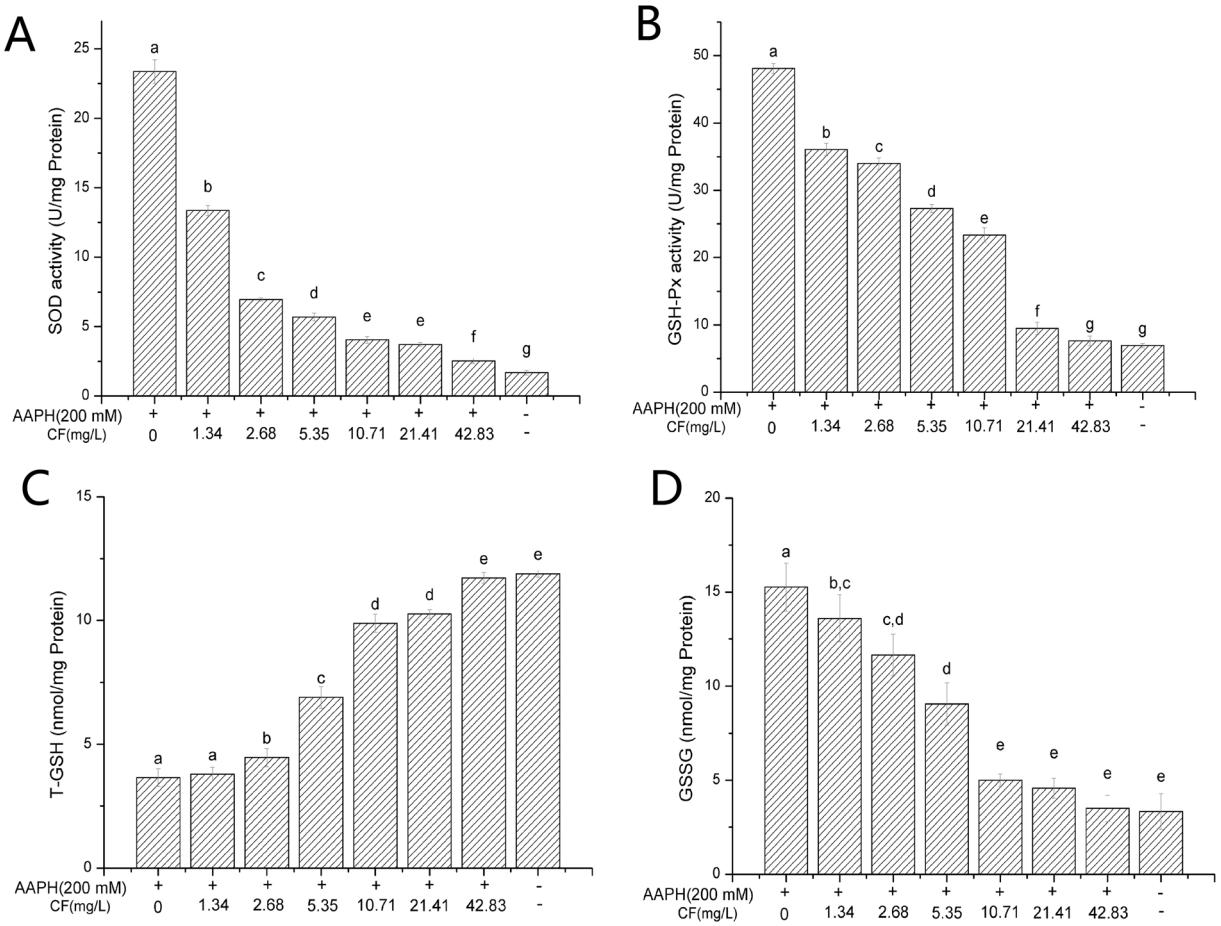

Fig. 6 Enzyme activities of SOD (A) and GSH-Px (B); amount of GSSG (C) and T-GSH (D) in human erythrocytes. Erythrocytes were pretreated with CF sample for 30 min prior to AAPH (200 mM) treatment for 2 h. Data are mean ± standard deviations of three independent experiments.

amounts of the extracted flavonoid compounds; various types of flavonoid compounds were extracted in different proportions with different pretreatments based on the method and parameters, especially the time and power.

3.4 Free radical scavenging capabilities of flavonoid compounds after different pretreatments

Many researchers have reported the great benefits of the antioxidative properties of flavonoid compounds.[35,36] In this study, we also assessed the free radical scavenging abilities of the flavonoid compounds after different treatments. Firstly, DPPH free radicals, ABTS free radicals, and ferric ions were employed and the results are shown in Fig. 4. Here, VC was treated as the positive control group, and all flavonoid groups showed remarkable antioxidative abilities to scavenge ABTS and DPPH free radicals in a dose–response manner whereas the same ability was lacking in ferric ions. The M400+U400 group (30 min) with high extraction efficiency resulting from the globular spatial structure showed significantly higher ABTS and DPPH free radical scavenging capabilities. The same tendencies were seen for the M400+U400 group (40 min) when compared with the other treatment groups. Many studies have reported the promising antioxidative effects of naringin, 2″-*O*-acetyl-3′-*O*-methylrutin, and 5,7,8,3′-tetrahydroxy-3,4′-dimethoxy flavone. For example, it has been reported that the antioxidant mechanism of naringin involves the reduction of the oxidative stress induced by AAPH.[36] Flavonoids containing catechol groups have stronger antioxidant capacity.[37] 2″-*O*-Acetyl-3′-*O*-methylrutin is one of the flavonols, and its antioxidant activity is related to the number of hydroxyl groups on the C ring.[38] The antioxidant mechanism of 5,7,8,3′-tetrahydroxy-3,4′-dimethoxy flavone has been rarely reported. However, the number of hydroxyl groups was positively correlated with the antioxidant activity whereas the number of methoxy groups was negatively correlated with it.[39]

At the cellular level, the AAPH free radical-induced hemolysis model was used and the results are shown in Table 2. The results reveal a positive relationship between the chemical and cellular antioxidative abilities in the same treatment group. For example, the M400+U400 group treated for 30 min or 40 min with significantly high *in vitro* antioxidative capabilities showed high scavenging ability for the AAPH free radical at the cellular level, which was much lower than the hemolytic rate (Fig. 4A and D respectively; Table 2). These results may be owing to the increasing concentrations of antioxidative flavonoid compounds obtained because of the steps taken to promote the extraction yield.

3.5 Structure of purified flavone fraction CF and its protective effects against AAPH-inducted erythrocyte hemolysis

In this study, we further purified the crude flavone fraction in the group M400+U400 (40 min) with high extraction efficiency using AB-8 macroporous resin. During the purification processing, the cCF sample was first washed with ultrapure water to remove the water-soluble impurities. As shown in s-Fig. 1 in the ESI,† the polysaccharide content was employed as an indicator to determine whether the water-soluble impurities had been removed completely. Moreover, s-Fig. 2 in the ESI† indicates that only one single fraction was detected when the sample was eluted with 40% ethanol solution. After collection and lyophilization, the purity of CF was 87.37 ± 0.97%; subsequently, the composition of this purified flavone fraction was characterized through PR-LCMS analysis and the result is presented in Table 3. As we can see, after purification, two types of flavones, genistein-7,4′-di-*O*-β-D-glucoside and (3*R*)-duartin (shown in s-Table 9†), disappeared; three flavones were found, namely naringin, 2″-*O*-acetyl-3′-*O*-methylrutin, and 5,7,8,3′-tetrahydroxy-3,4′-dimethoxy. Furthermore, the AAPH-induced hemolysis model was used to assess the antioxidative capability of CF and the results are shown in Fig. 5 and 6. It can be seen that CF had remarkable protective effects on the erythrocytes by decreasing the rate of hemolysis. Fig. 5A highlights the dose–response manner of CF in inhibiting the rate of erythrocyte hemolysis. Especially, there was no significant difference ($p < 0.05$) between the groups treated with 42.83 mg mL^{-1} CF and the control group. In our previous study, the erythrocyte protection mechanism of flavonoids was explained by the fact that the antioxidative effects of flavonoid compounds directly quenched the AAPH free radicals inside the erythrocytes and therefore decreased the antioxidative-associated enzyme level and the metabolites.[40] Especially, the low content of MAD, facilitated by the antioxidative properties of flavonoid compounds, decreased the lipid peroxidation of the cytomembrane and therefore superficially characterized the decrease in hemolysis.[41,42] In this study, we found that the MDA (Fig. 5B), hydrogen peroxide (Fig. 5D), and GSSG (Fig. 6D) contents, and the enzyme activities of LDH (Fig. 5C), SOD (Fig. 6A), and GSH-Px (Fig. 6B) decreased whereas the T-GSH content increased (Fig. 6C) with an increase in the CF content, indicating that CF could quench the AAPH free radicals and function in a manner similar to the above pathway in which CF acted as the AAPH free radical scavenger to lower the reactive oxygen species (ROS) level in the erythrocytes, thereby decreasing the enzyme activities of SOD, LDH, and CAT, as well as the MDA content. As a result, we could infer that CF with relatively high flavone purity had a greater possibility of quenching the AAPH free radicals (as shown in Fig. 3C), which agreed with the conclusion of our previous study.[40]

4. Conclusions

Pomelo is a fruit traditionally grown in Lingnan and is popular in China, especially in Guangdong Province. Due to its excellent flavor and high nutritive value, pomelo is currently exported across Asia, and to the United States, Canada, Europe, and other countries. Pomelo fruitlet is the immature pomelo fruit, which is a side-product of the pomelo crop. In this study, ultrasonic-associated microwave extraction was conducted to obtain the flavonoid compounds from pomelo fruitlets with high extraction efficiency and strong free radical scavenging capabilities. Through different pretreatments, we found that microwaves may induce the formation of globular shapes, the processing time and temperature having a positive effect on the percentage of globule formation; ultrasonic treatment was able to facilitate the formation of a curved surface, which may block the formation of globules during subsequent treatment with microwaves. The extraction efficiency analysis revealed that ultrasonic treatment associated with microwaves significantly increased the extraction yield of the flavonoid compounds when compared with the sequential treatment of ultrasonic waves and microwaves, in which the synergetic effects were able to facilitate the breaking down of the cell wall. Through PR-LCMS analysis, the types of flavonoid compounds present in all groups were identified and the results indicated a weak relationship between the extraction yields and the number of flavonoid types. Therefore, a suitable method with certain parameters is needed to collect the intended flavonoids. With regard to the antioxidative capabilities, all groups showed great DPPH and ABTS free radical scavenging abilities in a dose–response manner. The free radical scavenging abilities were investigated using the AAPH-induced hemolytic model, in which the ultrasonic-microwave synergetic groups showed significantly higher *in vitro* performance and cellular-level antioxidative capabilities and bioavailability. Furthermore, we purified the flavone fraction by using AB-8 macroporous resin from the M400+U400 group treated with ultrasonic waves (400 W) combined with microwaves (400 W) for 40 min. Three flavones, namely naringin, 2″-*O*-acetyl-3′-*O*-methylrutin, and 5,7,8,3′-tetrahydroxy-3,4′-dimethoxy, were identified, which were able to quench the AAPH free radicals, thereby decreasing the ROS level in erythrocytes and inhibiting hemolysis. This study may provide some useful information on increasing the utilization of pomelo and determining the optimum ultrasonic and microwave methods to perform flavonoid extraction.

Funding

This study was funded by Guangdong Key Laboratory of Agricultural Products Processing, Guangzhou Science and Technology Program of China (project no. 201704030084), the Guangdong Science and Technology Program of China (project no. 2016A040402045).

Conflicts of interest

None.

References

1 J. B. Harborne and C. A. Williams, *Phytochemistry*, 2000, **55**, 481–504.

2 T. Wu, Y. Guan and J. Ye, *Food Chem.*, 2007, **100**, 1573–1579.
3 M. Zhang, C. Duan, Y. Zang, Z. Huang and G. Liu, *Food Chem.*, 2011, **129**, 1530–1536.
4 W. Xi, B. Fang, Q. Zhao, B. Jiao and Z. Zhou, *Food Chem.*, 2014, **161**, 230–238.
5 P. R. Chaudhary, G. K. Jayaprakasha, R. Porat and B. S. Patil, *Food Chem.*, 2014, **153**, 243–249.
6 P. R. Chaudhary, G. K. Jayaprakasha and B. S. Patil, *Food Chem.*, 2015, **188**, 77–83.
7 J. J. Daniel, D. K. Owens and C. A. Mcintosh, *Phytochemistry*, 2011, **72**, 1732–1738.
8 A. Lers, S. Burd, E. Lomaniec, S. Droby and E. Chalutz, *Plant Mol. Biol.*, 1998, **36**, 847–856.
9 R. M. Uckoo, V. M. Balasubramaniam and B. S. Patil, *J. Food Sci.*, 2012, **77**, C921–C926.
10 K. K. Chebrolu, J. Jifon and B. S. Patil, *Food Chem.*, 2016, **196**, 374–380.
11 J. Juskiewicz, Z. Zdunczyk, M. Wroblewska, J. Oszmianski and T. Hernandez, *Food Res. Int.*, 2002, **35**, 201–205.
12 K. Fukuda, T. Ohta and Y. Yamazoe, *Biol. Pharm. Bull.*, 1997, **20**, 560.
13 M. A. Berhow and C. E. Vandercook, *Phytochemistry*, 1989, **28**, 1627–1630.
14 W. R. Raymond and V. P. Maier, *Phytochemistry*, 1977, **16**, 1535–1539.
15 D. L. G. Al, U. Etxeberria, A. Haslberger, E. Aumueller, J. A. Martínez and F. I. Milagro, *J. Med. Food*, 2015, **18**, 890.
16 S. U. Mertens-Talcott, I. Zadezensky, W. V. Castro De, H. Derendorf and V. Butterweck, *J. Clin. Pharmacol.*, 2013, **46**, 1390–1416.
17 W. N. Zou, W. Wang, X. U. Qi-Jiang, D. U. Wei-Wei and L. I. Ling-Yu, *Sci. Technol. Food Ind.*, 2017, **38**, 266–271.
18 H. Dejian, O. Boxin and R. L. Prior, *J. Agric. Food Chem.*, 2005, **53**, 1841–1856.
19 K. Fröhlich and V. Böhm, *Food Chem.*, 2011, **129**, 139–148.
20 H. W. Ding, *J. Nucl. Agric. Sci.*, 2013, **27**, 329–333.
21 D. W. Zhu, P. X. Yue, J. X. Wang, D. S. Yuan and Y. S. Chen, *Trans. Chin. Soc. Agric. Mach.*, 2010, **41**, 136–140.
22 S. Chemat, H. Aït-Amar, A. Lagha and D. C. Esveld, *Chem. Eng. Process.*, 2005, **44**, 1320–1326.
23 P. R. Birkin, D. G. Offin and T. G. Leighton, *Phys. Chem. Chem. Phys.*, 2005, **7**, 530–537.
24 M. Liu, M. Kong, Z. Liu, F. Zhang and D. Chen, *Food Sci.*, 2016, **37**, 74–80.
25 A. Leone, A. Tamborrino, R. Romaniello, R. Zagaria and E. Sabella, *Biosyst. Eng.*, 2014, **125**, 24–35.
26 T. Wang, W. Li and T. X. Li, *Key Eng. Mater.*, 2017, **737**, 7.
27 Y. H. Guo, H. Zheng, H. Zhang, L. Y. Ma, J. Han and K. Li, *Appl. Mech. Mater.*, 2012, **161**, 6.
28 Z. X. Q. Kangquan and L. Xin-lu, *Med. Plant*, 2011, **2**, 51–53.
29 P. C. Ho, D. J. Saville and S. Wanwimolruk, *J. Pharm. Pharm. Sci.*, 2001, **4**, 217–227.
30 U. Fuhr and A. L. Kummert, *Clin. Pharmacol. Ther.*, 1995, **58**, 365–373.
31 S. Rainer and M. Rolf, *J. Nutr.*, 2006, **136**, 1477.
32 Y. Masayuki, M. Toshiyuki, I. Tomoko, M. Toshio, K. Masatomo, H. Yoshihiko and M. Hisashi, *J. Nat. Prod.*, 2002, **65**, 1151–1155.
33 H. W. Lu, K. Sugahara, Y. Sagara, N. Masuoka, Y. Asaka, M. Manabe and H. Kodama, *Arch. Biochem. Biophys.*, 2001, **393**, 73–77.
34 F. Torres, J. Quintana and F. Estévez, *Mol. Carcinog.*, 2010, **49**, 464–475.
35 N. Li, J. H. Liu, J. Zhang and B. Y. Yu, *J. Agric. Food Chem.*, 2008, **56**, 3876–3883.
36 M. Byung-Sun, T. C. Van, D. Nguyen Tien, D. Nguyen Hai, J. Han-Su and H. Tran Manh, *Chem. Pharm. Bull.*, 2010, **40**, 1725–1728.
37 M. M. Silva, M. G. Santos, R. Rocha, G. Justino and L. Mira, *Free Radical Res.*, 2002, **36**, 1219–1227.
38 R. C. T. Ghiotto, F. C. Lavarda and F. J. B. Ferreira, *Int. J. Quantum Chem.*, 2004, **97**, 949–952.
39 O. L. Woodman and W. M. Meeker, *J. Cardiovasc. Pharmacol.*, 2005, **46**, 302–309.
40 W. Hui, H. Xi, F. Lai, J. Ma and H. Liu, *RSC Adv.*, 2018, **8**, 12116–12126.
41 L. Ma and G. Liu, *J. Agric. Food Chem.*, 2017, **65**, 11320–11328.
42 L. Ma, G. Liu and X. Liu, *Int. J. Food Sci. Technol.*, 2011, **2**, 51–53.